

The Novel ABALONE Photosensor Technology¹

Daniel Ferenc^a, Andrew Chang^a, and Marija Šegedin Ferenc^b

(a) Physics Department, University of California, Davis
One Shields Ave., Davis, CA-95616, USA

(b) PhotonLab, Inc., 3315 Oyster Bay Ave., Davis, CA-95616, USA

ABSTRACT

The patented and proven ABALONE Photosensor Technology (Daniel Ferenc, U.S. Patent 9,064,678, 2010) has the capability of opening new horizons in the fields of fundamental physics, functional medical imaging, and nuclear security. The exceptionally simple ABALONE Photosensor design comprises only three vacuum-processed components, each made of glass. Through avoidance of all materials other than glass, we have bypassed an ‘Old-Technology Barrier,’ which has prevented the extremely expensive ($> \$100\text{k}/\text{m}^2$) photomultiplier tubes (PMTs) and all of the other vacuum photosensor concepts from evolving into a modern vacuum technology. This article discusses our new technology and overviews the unprecedented performance of ABALONE Photosensors, produced in the custom-designed production line at UC Davis and continuously tested since 2013. In conclusion, the modern ABALONE Technology is far superior to prior art in performance, robustness and the capacity for integration into large-area detector shells. It is about two orders of magnitude more cost effective while being mass-producible with a relatively low investment.

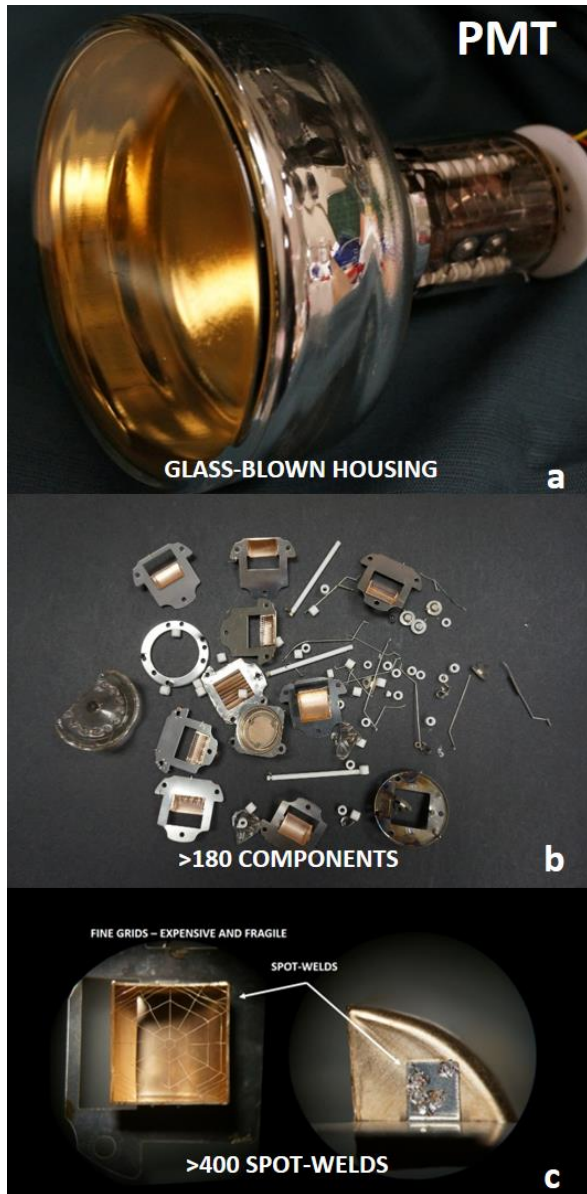
KEYWORDS: photosensor, vacuum, imaging, medical, neutrino, gamma-ray

1. INTRODUCTION

The novel ABALONE Photosensor Technology [1] has the capability of supplanting the expensive 80-year-old Photomultiplier Tube (PMT) manufacture by providing a modern and cost-effective alternative product, thus opening new horizons in all application areas, including large experiments in fundamental physics, as well as new types of scanners for both functional medical imaging and nuclear security [2].

Up to this point, the broad field of large-area photon detection has been virtually stuck with the extremely expensive ($> \$100,000/\text{m}^2$) vacuum PMT manufacture (Fig.1, Fig.2(a,b)).

¹ Submitted for publication to Nuclear Instruments And Methods In Physics Research A on March 12, 2017 (Ms. Ref. No.: NIMA-D-17-00243).



Additionally, the millimeter-sized all-silicon devices, particularly the Geiger-Mode Avalanche Photo Diodes (G-APDs) (somewhat pretentiously and inaccurately called Silicon Photo Multipliers² (SiPMs)) are and will remain far too expensive (currently ~\$10 million/m²) for any truly large-area application.

Paradoxically, in contrast to the makers of PMTs, many modern industries that are also based on vacuum processing technologies have been thriving with the production of numerous items, ranging in complexity from blank compact discs (CDs) (<\$10/m²) to plasma and other flat TV screens (~\$500/m²). Our detailed studies led to the clear conclusion that the reason why the PMT manufacture could never have evolved into such a modern, cost-effective vacuum technology is simply intrinsic to its very concept—it lies in the combination of materials that the PMTs are made of (Fig.1, Fig.2(a,b)). For the reasons discussed below, that combination necessitates a daylong static vacuum bakeout, which precludes any form of modern, continuous-line production, resulting effectively in an insurmountable ‘Old-Technology Barrier.’

Fig.1 The anatomy of a Photomultiplier Tube. The ‘Old-Technology Barrier’ has prevented the 80-year old PMT manufacture from making progress. Part of the problem has been in the number of hand-made components (a, b) and the assembly processes (c), but the real, intrinsic and insurmountable problem is in the combination of materials that enforces vacuum-cleaning in a long, static bakeout at a compromise temperature.

² The signal-amplification process in these sensors goes via electron-hole pair multiplication, rather than photon multiplication. The effect of photo-multiplication nevertheless takes place as a side effect, and causes one of the main drawbacks of G-APDs – the photon crosstalk. The term ‘photo multiplier tube’ was an incorrect choice for the PMTs in first place.

Every bakeout within a pumped vacuum environment is a statistical process, characterized by a trade-off between the temperature and the bakeout time. The presence of glass among the inseparable PMT components limits the maximum bakeout temperature far below the optimal outgassing temperatures for metals and ceramics. The trade-off must occur at the expense of the bakeout time, which then causes the ‘Old-Technology Barrier.’

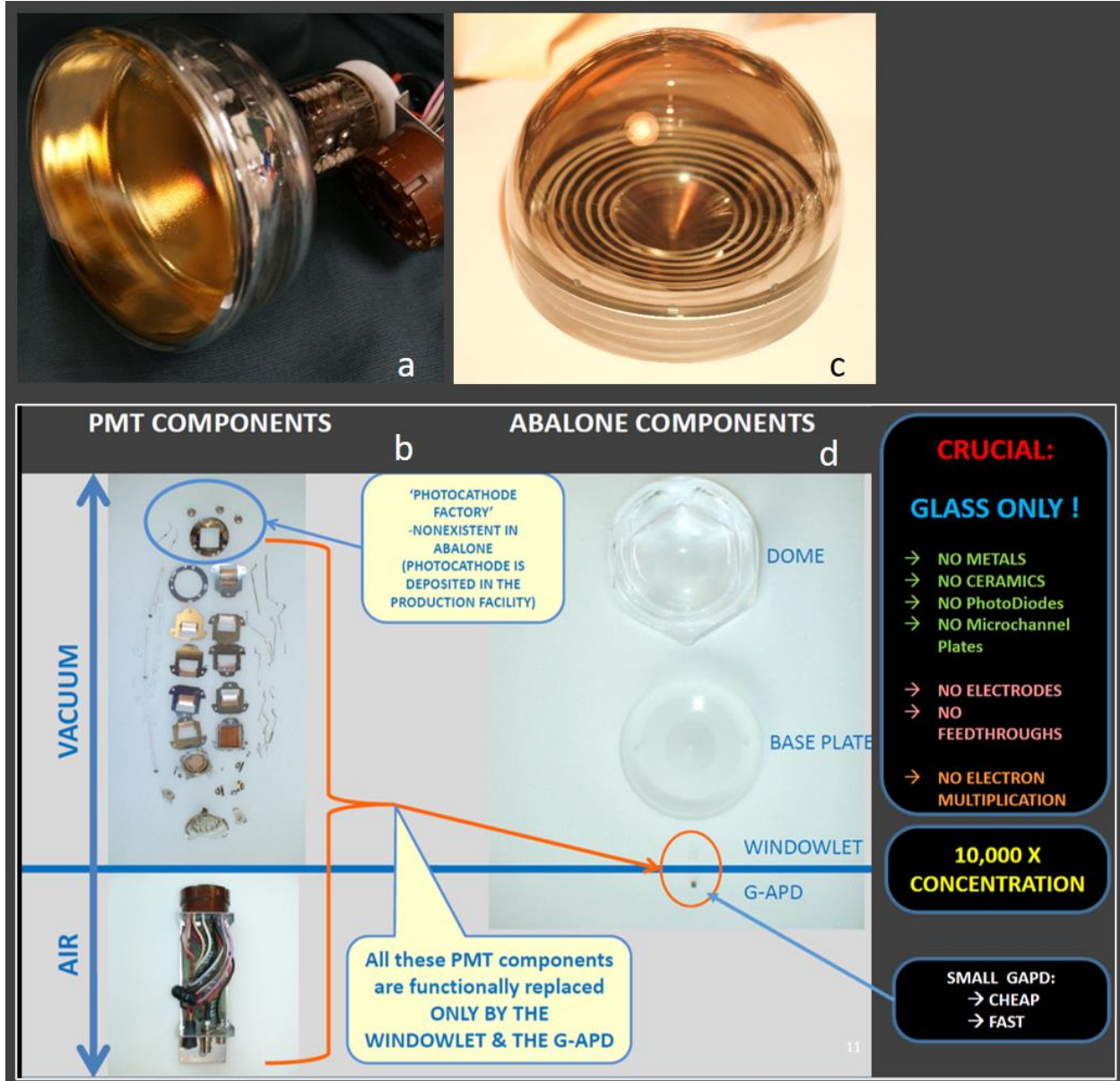


Fig.2 A PMT (a), and its components (b); more than 180 hand-made components; about 10 materials; more than 400 spot-welds (Fig.1); evaporators of photocathode-building materials remain in the PMT. The ABALONE Photosensor [1] (c) and its components (d); only 3 glass vacuum-processed components, treated in a way equivalent to the production of CDs; assembly—patented mass-production technology. The ultimate simplicity translates into unprecedented performance and about two orders of magnitude lower production cost.

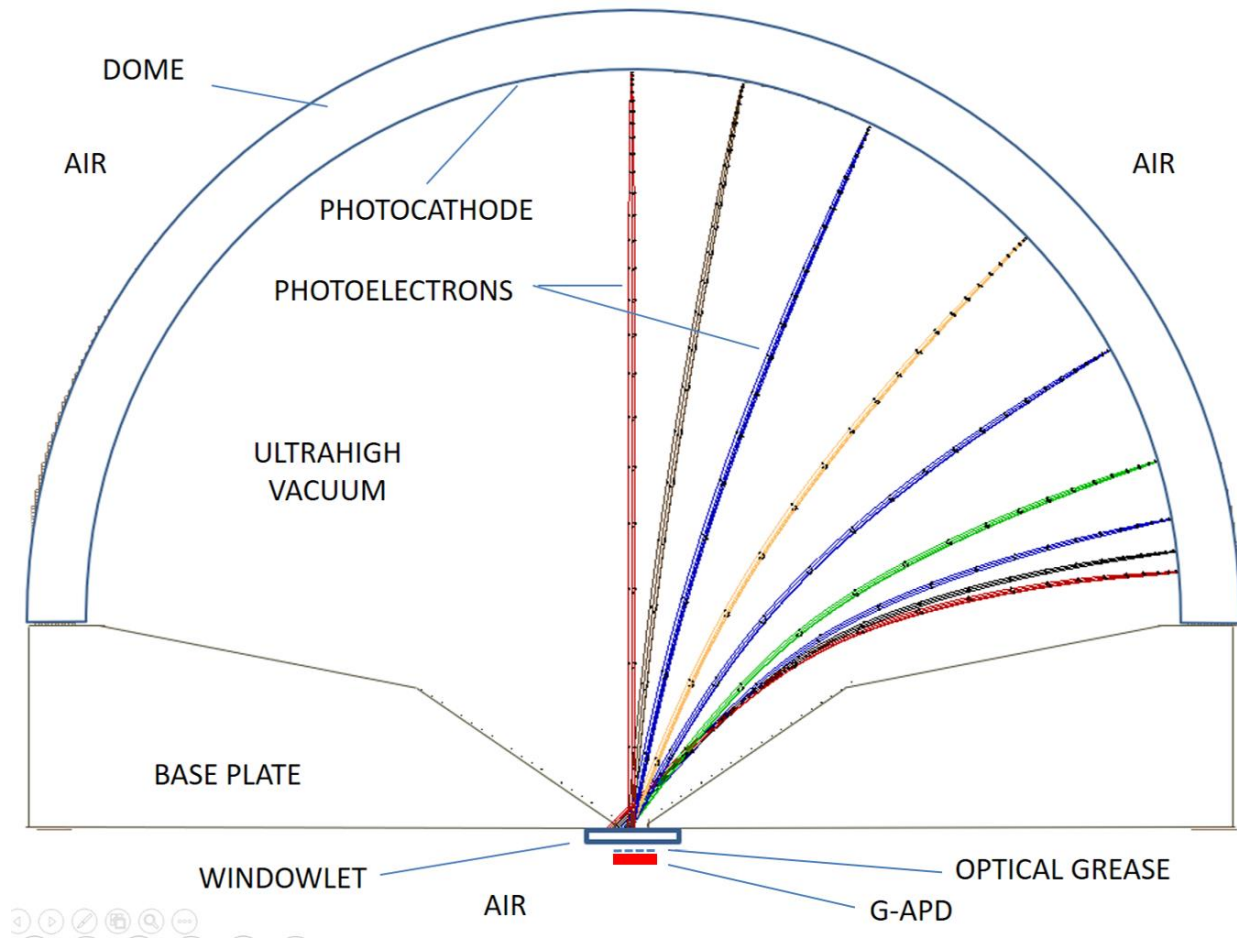


Fig. 3 Schematic view of the ABALONE Photosensor [1]. The electron trajectories are the results of the simulations of 20 keV electrons with a 0.25 eV transverse energy spread, for a Dome of a 10 cm inner diameter. The concentration factor from the photocathode area to the readout area is $\sim 10,000$. A Geiger-Mode Avalanche PhotoDiode (G-APD) is optically coupled to the airside of the Windowlet to detect secondary photons created in impacts of photoelectrons in the Windowlet-scintillator.

Unlike metals or ceramics, glass does not release trapped gases from its bulk at the temperatures of interest, so it does not need a deep bakeout, but rather just a surface-layer scrub [3]. Consequently, in stark contrast to PMTs and all of the other previously considered vacuum photosensor concepts, we have bypassed the ‘Old-Technology Barrier’ through the highly non-trivial avoidance of all materials among the vacuum-processed components, other than glass [1]. The exceptionally simple ABALONE Photosensor design—unique in enabling this new technology—comprises only three industrially pre-fabricated (e.g. molded) glass components (Fig.2 (c,d), Fig.3, Fig.4). These three glass pieces enter a continuous production-line process, which starts with a standard rapid plasma cleaning (i.e. a surface scrub without a long bakeout), continues with a standard rapid thin-film deposition process, and ends with hermetic bonding of the three components, when the two thin-film seals between them are activated. Our modern production method is thus virtually equivalent to the mass-production of blank compact discs (CDs). Note that the two sealing surfaces are made of one of the deposited thin-films—the multi-functional smart alloy invented in the UC Davis Ferenc-Lab in 2004 [4].

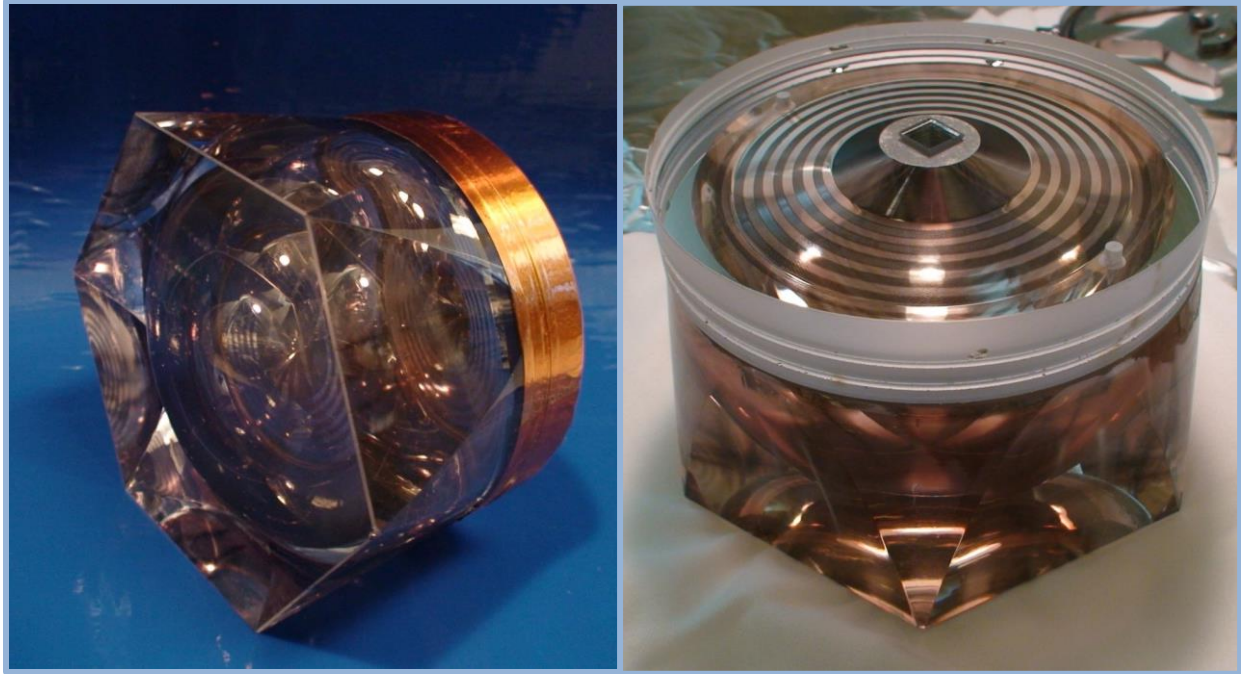


Fig. 4 The results presented in this publication are based on the tests of the shown ABALONE photosensor, continuously tested ever since its assembly in May 2013.

The low production cost is accompanied by uniquely simple integration methods. For example, ABALONE Photosensors may be integrated within thin and lightweight panels, serving as modules for ultrasensitive whole-body-enclosing ($\sim 20\text{m}^2$ of sensitive area) medical PET scanners that can provide a virtually harmless (ultra-low-dose) cancer-screening of a general, symptom-free population [2]. The same underlying invention enables custom-shaped detectors of illicit radioactive materials, or detectors for cosmic rays, cosmic gamma rays, neutrinos and dark matter. In all cases, these self-supporting detector shells can be assembled in the field, from the encapsulated, vibration and shock proof, cable-free, electrically shielded and waterproof panels that seamlessly lock to each other [2].

Yet another unique advantage of the ABALONE Technology that comes directly from its simplicity, is the unprecedentedly low level of radioactivity [1]. This comes naturally when all three, or at least the two large components of an ABALONE Photosensor are made of ultrapure fused silica, like in the case presented in Fig.4.

Note that the other vacuum photosensor concepts—Smart-PMTs, the Hybrid Photo-Diodes³ (HPDs) and the PMTs based on microchannel plates (MCP-PMTs)—have all been inhibited by the very same “barrier” like the PMTs, because their manufacturing processes necessitate the same, and even more problematic components, like silicon photo-diodes (SiPDs) and microchannel

³ Hybrid photo-diodes are by definition vacuum photosensors in which a silicon photo-diode is directly exposed to photoelectrons, so the photo-diode must be mounted within the vacuum enclosure.

plates (MCPs). SiPDs are much more sensitive to heat than glass, which even further limits the bakeout temperature and prolongs the bakeout time. They must be specially prepared for the implementation in HPDs, to prevent ‘poisoning’ with traces of alkali vapors from the photocathode, which increases the cost by a large margin. Furthermore, SiPDs are extremely sensitive to static electricity and strong field gradients, which are likely to occur in large-scale applications. On the other hand, MCPs naturally absorb large amounts of gas within their microscopic multiplication channels (the total surface area encapsulated in a small MCP-PMT is on the order of 10m^2 , while the cross section of a single channel is $\sim 10^{-12}\text{m}^2$). Thus, even an extremely long vacuum-bakeout is insufficient, and it must be accompanied by low-intensity electron bombardment, or ‘electron brushing’ (strong electron fluxes must not be applied, since they would damage the MCPs).

So far, ABALONE Photosensors have been produced only in the specially constructed ABALONE Prototype Pilot Production Plant (A4P) (part of the Ferenc-Lab at UC Davis), which is in essence a downscaled version of a real production line, but nevertheless performs all of the processes accurately. PhotonLab, Inc. has acquired a significantly more advanced production facility, as well as the testing and evaluation laboratory that has been used in the hereby presented analysis.

This article is the first report on the continuous, 3.5-year long performance tests of the ABALONE Photosensors. We will discuss the following key performance aspects: vacuum integrity and afterpulsing, timing resolution, single-photon sensitivity and resolution, and photoelectron back-scattering.

Separate publications will report on in-depth studies of the discussed topics, as well as a number of other important subjects, including thermionic noise and performance at ultralow temperatures, performance with a new generation of G-APDs and scintillators, the unprecedented radioactive cleanliness for applications in dark matter search, modular panels, and the specially designed ABALONE Photosensors for neutrino physics.

2. THE ABALONE PHOTODIODE

Fig.3 shows a schematic view of the ABALONE Photosensor. It comprises only three vacuum-processed components, each of which is made of glass. Two glass-to-glass bonds are established using our *smart multi-functional thin-film material*, one between the Dome and the Base Plate, and the other between the Base Plate and the Windowlet. Our novel bonding and vacuum encapsulation method [4] has been thoroughly tested and optimized ever since its conception in 2004. We have fine-tuned the latest generation of seals for the very small sealing surfaces between the Windowlet and the Base Plate, and particularly for their mechanical strength. Destructive pulling tests have demonstrated that the seals never decouple, but rather, the bulk glass material breaks around, or underneath the bonded areas.

These two conductive bonds play another key role: they pass the high voltage (between the Dome and the Base Plate), and the ground potential (between the Base Plate and the Windowlet), into the evacuated volume. This allows the ABALONE Photosensor to function without any

through-the-glass feedthroughs, i.e. without any metals among the vacuum-processed components. Recall that the absence of metals among the components is key to the ABALONE Technology.

Each photoelectron emerging from the photocathode on the inside surface of the Dome is focused and accelerated into the small hole in the center of the Base Plate. Practically all photoelectrons enter that hole, independently of the origination point, except for a small fraction ($\sim 10^{-4}$) of those that are significantly deflected in rare collisions with residual gas constituents. The photoelectron collection efficiency of ABALONE Photosensors is thus practically 100%. The hole in the Base Plate is covered and vacuum-sealed by the Windowlet (Fig.2 (d), Fig.3, Fig.4) from the outside. The concentration factor from the photocathode area to the bombarded Windowlet area is 10,000, which minimizes the G-APD area, and thus the overall cost. For instance, a detector of $\sim 1\text{m}^2$ area, composed of closely packed ABALONE Photosensors [2], would require only $\sim 1\text{cm}^2$ of total G-APD area. The small size of each individual G-APD's area directly translates into a small capacitance and resistance, i.e. it assures fast timing resolution.

On its vacuum-side, the Windowlet is coated with a multifunctional thin-film alloy, which: (i) provides a conductive coating over the photoelectron-receiving surface, (ii) connects that surface to the ground potential on the air-side of the photosensor, (iii) participates in the vacuum encapsulation process, in conjunction with the smart multifunctional thin-film coating, (iv) acts as a reflector, directing photons created in the scintillator towards the G-APD, and thus also (v) prevents secondary photons from reaching the photocathode. The Windowlet can either be entirely made of a suitable scintillator material, or as a thin glass plate coated on its vacuum-facing surface with a thin scintillator film ($< 2\mu\text{m}$). The Windowlet-scintillator converts the kinetic energy of the accelerated photoelectrons into secondary photons, which are then detected by the G-APD.

When a photoelectron hits the surface of the Windowlet exposed to vacuum, it first penetrates the thin-film of alloy in which it loses a certain amount of energy. While electrons of 2.5 keV lose virtually all of their energy, electrons of 20 keV lose only about 0.3 keV, because the rate of energy loss in matter for electrons of these energies is inversely proportional to the kinetic energy [5]. The remaining energy allows each photoelectron to penetrate deep into the scintillator ($< 2\mu\text{m}$), where it generates a large number of secondary photons, proportional to its kinetic energy and the scintillator yield.

The ABALONE Technology clearly belongs to a class of its own. Regarding the light detection principle, ABALONE Photosensors just vaguely belong to the class of Image Intensifiers, and rather accurately to a separate class, which we have previously defined as Light Amplifiers [6, 7]. We came up with that term in order to underline the key distinctive feature: light amplification, but without imaging. The other two differences are the speed of the generation of secondary photons (scintillator vs. phosphor) and the specific method of detection (G-APD vs. CCD, or the naked eye). However, a G-APD in an ABALONE Photosensor can be replaced with other sensors, such as an analog APD, a PiN diode, a miniature CCD, or even the naked eye. We have used the last two methods in stress tests of the ABALONE Photosensors by exposing them briefly to strong sources of light, including daylight. Indeed, a bright spot on the air side of the Windowlet was clearly visible. The absence of light-induced damage, along with manifest mechanical robustness and overall simplicity of the ABALONE Photosensors, makes them uniquely robust and safe.

3. EXPERIMENTAL

The Dome of the ABALONE Photosensor used in our tests (see Fig.4) has a hexagonal shape on the outside (an approximation to the Winston cone for close packaging into arrays), and is made of fused silica. A hemispherical one, made of borosilicate glass, is shown in Fig.2(c). Any photocathode can be grown in the Dome under fully controlled conditions within the production system. For this study, we chose the S11 photocathode (Cs_3Sb), because it spontaneously converges to the optimal stoichiometric configuration. (This makes it ideal for R&D projects focusing on topics other than the photocathode.)

The Windowlet is a $6 \times 6 \times 1.5 \text{ mm}^3$ plate made of the LYSO scintillator material (Cerium-doped Lutetium Yttrium Orthosilicate). We chose LYSO for this study because of its mechanical and chemical robustness, rather than its yield or speed. Some other scintillators that offer much better performance than LYSO have also been studied recently, but the results presented in this article clearly show that an ABALONE Photosensor with a LYSO scintillator already provides an outstanding performance for most applications. The optical coupling of the G-APD to the Windowlet was done with standard optical grease rather than a permanent optical cement, at the expense of light-transmission efficiency, because that allowed us to test so far seven different G-APDs from different manufacturers. The possibility of replacing G-APDs at any time is yet another important intrinsic advantage of the ABALONE concept. The data presented in this article were all taken with a $3 \times 3 \text{ mm}^2$ SensL J-type MicroFJ G-APD that comprises $35 \mu\text{m}$ cells.

A 23keV photoelectron generates an estimated 600 photons in the LYSO scintillator. About 40-100 of them get recorded, depending on the G-APD model and bias voltage. The latter estimate came from precise counting of the individual photons, resolvable in the fast signals of the SensL J-type G-APD (to be published separately). Our 1-photoelectron signal (~ 55 secondary photons) therefore dwarfs the G-APD noise, and guarantees excellent single-photon sensitivity and resolution.

We applied a negative, ultra-low current high-voltage on the photocathode, while the Windowlet and the attached G-APD were shielded within a grounded conductive miniature cylinder that forms a Faraday cage together with the Windowlet and the sealing surface around it. The ABALONE Photosensor consumes practically no power. A high-voltage power supply similar to the miniature supplies in night-vision goggles can be used, but still of a significantly lower power. The acceleration potential can range between approximately 4kV and 25kV (successful tests went up to 30kV), depending on the application. A 405 nm LED light source was pulsed at 100 kHz, and all the hereby-presented data were gated. We have used a digital 5GHz LeCroy oscilloscope for data taking and analysis, directly connected to the G-APD output with a coaxial 50Ω cable, with SMA connectors.

4. RESULTS

4.1. VACUUM QUALITY AND AFTERPULSING

The presence of residual gas in any photocathode-based vacuum photosensor is critical, because it both inevitably leads to the ion-feedback afterpulsing noise, and harms the photocathode by ion impacts and chemical contamination. Our studies show that the afterpulsing rate of the ABALONE Photosensor is about two orders of magnitude lower than that of the proclaimed best PMTs [8]. Below, we discuss how this unique achievement is of a fundamental nature and intrinsic to the ABALONE Photosensor concept.

We will first discuss the diagnostic tool that we have used to constantly monitor the vacuum quality and the chemical composition of residual gas. An ABALONE photosensor may function as a rather precise time-of-flight (TOF) mass spectrometer for ions generated within its own vacuum. A fraction of about 10^{-4} of all photoelectrons in the ABALONE Photosensor ionize a neutral atom or a molecule on their way towards the scintillator (Windowlet). Each of those ions is then accelerated towards the photocathode, where secondary electrons may emerge upon its impact. Those electrons are detected the same way as photoelectrons, unless they miss the Windowlet due to an excessive initial transverse momentum. Their detection corresponds to the afterpulse, i.e. the “stop” signal in the ion TOF measurement, while the “start” signal comes from the detection of one or more of the initial photoelectrons. The time of flight of an ion is the time difference between the “stop” and the “start” signals, corrected for the electron’s flight time. The TOF spectrum in Fig.5 features peaks corresponding to ions of different masses and charge states. We have fitted a sum of Gaussian functions to TOF spectra, where each Gaussian function corresponds to an ion. We set the initial TOF values to the results of numerical simulations, assuming for simplicity that all ions originate from the Windowlet surface. For most of atoms and molecules other than noble gases at room temperature, that assumption is partly true, because they are in thermal equilibrium between their free and adsorbed states.

The afterpulsing rate has been of the order of 10^{-4} , and below 10^{-5} per photoelectron, for after-pulses of amplitudes higher than roughly 0.75 photons, and 4 photons, respectively. That is about two orders of magnitude lower than the rate in the proclaimed best PMTs [8] (when a factor 3 difference in the sizes of the sensors is taken into account). This is not surprising, given the fundamental differences in the production technologies as well as in the operation principles.

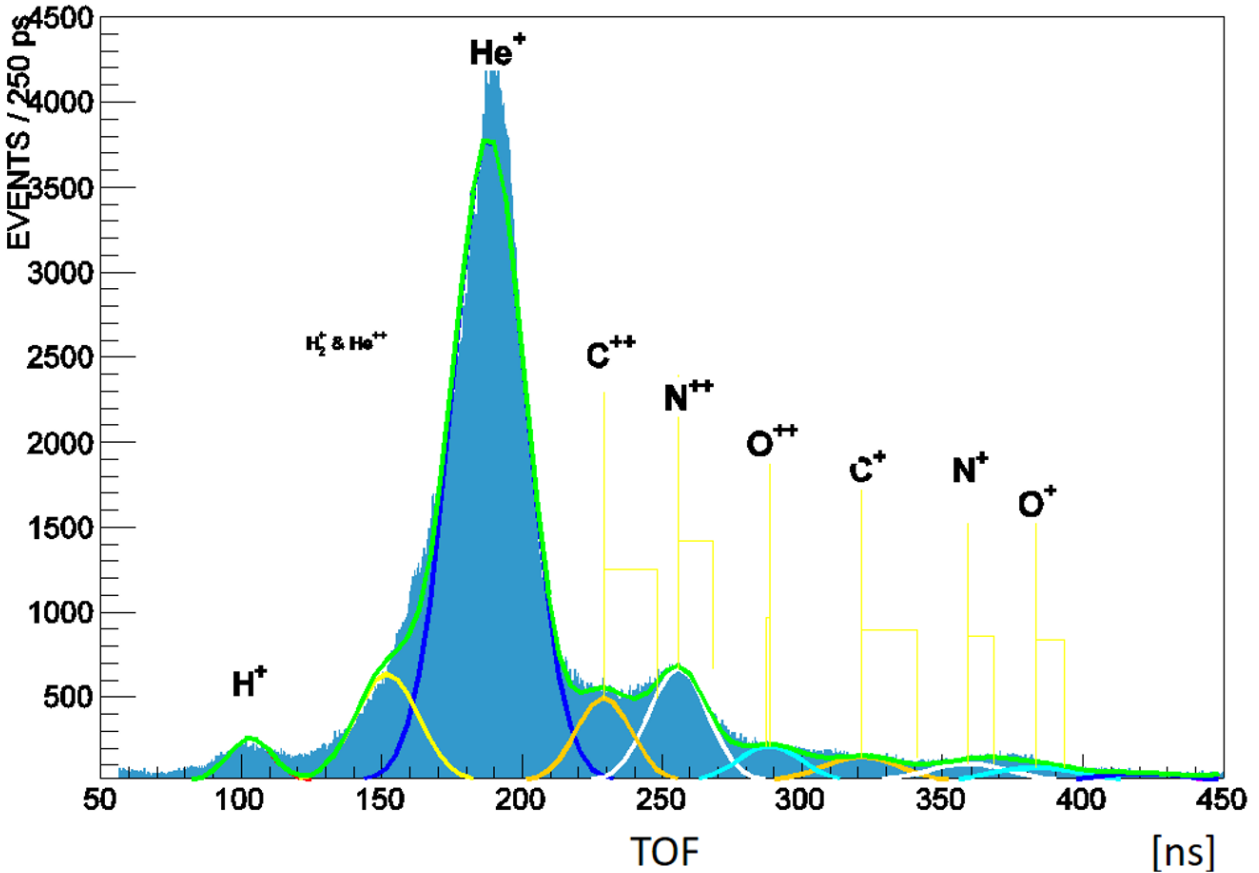


Fig.5 Time-of-flight mass spectrum of residual gas within the ABALONE Photosensor, operated at an acceleration potential of 20kV. Short vertical lines indicate the numerically predicted TOF values assuming that the ionization is taking place on the surface of the Windowlet, which served as the initial values in the fitting. The long vertical lines correspond to the best overall fit.

The initially observed traces of C, N, O, CO/N₂, CO₂, H₂O and Ar have dropped exponentially during the course of our continuous test, while the presence of He has remained constant, consistent with the fact that for any vacuum enclosure exposed to air, helium penetrates glass until its pressure reaches the partial atmospheric pressure. It may seem puzzling that the ABALONE Photosensor features an afterpulsing rate that is two orders of magnitude lower than that of PMTs, while the helium pressure is the same in both vacua. However, one should recall that ABALONE uses two orders of magnitude higher potential to accelerate photoelectrons, and that the ionization stopping power is inversely proportional to electron's kinetic energy [5]. Due to their two orders of magnitude higher energies, photoelectrons in ABALONE simply ionize two orders of magnitude less helium than the photoelectrons in PMTs⁴. This fundamental and irreducible advantage also holds for the other constituents of residual gas. Those ions appear only in traces, at

⁴ Note that ion gages and mass spectrometers, which benefit from maximizing the ionization probability, use electrons of practically the same energy as PMTs.

much lower partial pressures than helium. This exceptional level of vacuum cleanliness comes because of the following key factors:

- The intrinsic cleanliness of the ABALONE Photosensor Technology (e.g. base pressure of 10^{-11} Torr),
- The absence of any outgassing components, such as metals, ceramics, feedthroughs, microchannel plates, silicon diodes,
- Complete absence of electron multiplication, and thus electron-induced desorption within the vacuum,
- The integrity of the two thin-film seals,
- Minimum area, open geometry and high molecular conductivity, and particularly
- The three internal vacuum pumping mechanisms that constantly improve the vacuum level in ABALONE:
 - Ion implantation (explained below),
 - Physisorption on passive surfaces (none of the surfaces within ABALONE, except of the small electron-receiving Windowlet area, suffer from any electron bombardment),
 - Chemisorption on the multi-functional, chemically reactive thin getter film that covers 90% of the projected Base Plate area.

In general, the interaction of an energized ion with a solid depends on the properties of the solid, the ion's energy, its atomic number, charge, and the angle of incidence. For light elements (from H to O), the stopping power comes as a superposition of the so-called 'nuclear' interaction (nucleus-nucleus Coulomb scattering), and the low-energy tail ($dE/dx \sim E^{1/2}$) of the 'electronic' stopping power peak (excitation and ionization of atoms) [9, 10]. At 20keV, a light ion experiences a rather low stopping power ($\sim 3\text{-}20\text{eV/atomic layer}$, from H to Ar), so it easily passes through the thin photocathode film ($\sim 15\text{nm}$) with enough energy left to penetrate deep into glass ($\sim 50\text{-}200\text{nm}$), where it stops.⁵ Once implanted in glass, practically all atoms except of helium remain trapped, never returning into vacuum. Ion implantation thus acts as a very efficient vacuum pump. For instance, we have observed traces of argon disappearing soon after we started testing an ABALONE photosensor. As a noble gas, argon may not be chemisorbed in a getter, and therefore ion implantation remains the only possible explanation for its removal.

In contrast to ABALONE, ions generated in PMTs gain energies of only up to about 200eV. The stopping power for ions below 500eV in any solid is so high that they come to an abrupt stop right on the surface. Hard 'nuclear' collisions dominate and the displacement of target atoms is common⁶. The entire ion's energy is thus transmitted in one, or just a few collisions with atoms in the photocathode surface. Some ions may stay chemisorbed, contaminating the critical surface layer of the photocathode, while the others return into vacuum. Note that the surface-potential-

⁵ Ion implantation is a widespread industrial technique used for doping of solids deeply under the surface, while making minimal damage to the surface and a number of sub-surface layers. The optimal ion energies for that process include the range of ion energies used with ABALONE.

⁶ To maximize the sputtering efficiency of argon ions in a plasma, thin-film deposition systems typically bias sputtering sources to a potential of -500V.

barrier of a photocathode largely determines its properties. Vacuum pumping through ion-implantation in glass is impossible. Furthermore, in PMTs and MCP-PMTs the electron-induced desorption is massive, since each of the 10^5 - 10^6 electrons participating in the multiplication process bombards a solid surface with energies near the ionization probability peak. In conclusion, the unprecedentedly low level of afterpulsing is of a fundamental nature and intrinsic to the ABALONE concept.

4.2. TIME RESOLUTION

Time resolution of a photosensor is the precision with which it can measure the arrival time of a light pulse. Fig.6 shows the distribution of time intervals between the periodic pulses triggering the LED light source, and the detection times of the resulting signals. The ABALONE Photosensor was operated at 23kV, with a $3 \times 3 \text{mm}^2$ SensL G-APD readout biased to 30.5V. Signals were analyzed directly by a 5GHz oscilloscope, without external amplification. The detection time was determined by an inbuilt oscilloscope function, effectively a constant fraction discriminator set to 15% of the peak height. The timing resolution is 856ps, expressed as the full width at half maximum (fwhm) of the distribution shown in Fig.6. The decay time of the LYSO scintillator is 40-45 ns, which may seem long compared to the resolution. However, the leading edge of each single-photoelectron signal is highly populated with secondary photons and thus well defined. Pairs of signals arriving closely within the extended LYSO decay tails may be therefore also resolved.

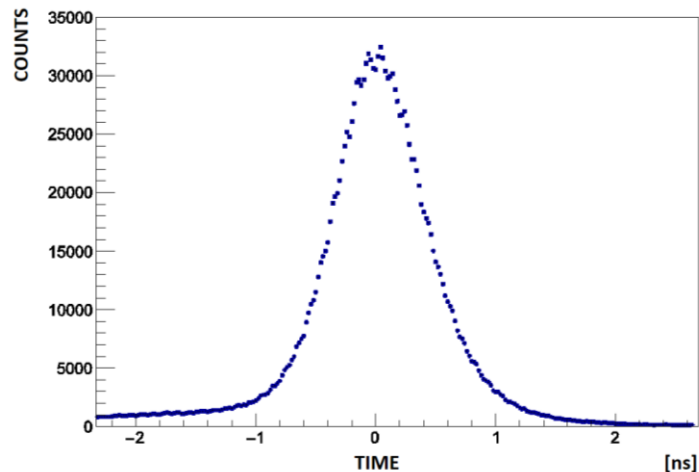


Fig. 6 The difference between the detection time of the single-photon signal, determined at a 15% signal fraction, and the trigger pulse for the 405 nm LED diode light source (the origin of the time scale shifted to the peak position). Time resolution, 856ps fwhm. The ABALONE Photosensor was operated at an acceleration potential of 23kV, with a $3 \times 3 \text{mm}^2$ SensL-J G-APD at a 30.5V bias. The light pulses used in this analysis were of the same intensity as shown in Fig..

The measured timing resolution comprises two trivial components: the jitter of the LED pulser (an estimated 500ps fwhm), and the systematic variation of the photoelectron's flight times with the distance of photon's conversion point on the photocathode, measured from the middle of the Dome. According to numerical simulations assuming normally incident light, the electron transit

time within the ABALONE Photosensor varies by 250ps—halfway from the center of the Dome—up to 550ps—between the center and the very edge of the Dome. This effect takes place because the current Dome shape is perfectly spherical, while the isochronous shape is slightly aspherical. Added in quadrature, these two effects already explain the observed resolution. This effect will diminish with the new generation of isochronous Domes. If the targeted time resolution falls below 100ps, isochronous ABALONE Photosensors of a smaller size should be used.

Further improvements of the time resolution are straightforward with the most recent generation of G-APDs, as well as faster scintillators. The sharp, strongly populated leading edge of the signal obtained with LYSO already provides an excellent time resolution for most applications, while at the same time it allows for the separation of close signals within the decay tail.

4.3. SINGLE-PHOTOELECTRON SENSITIVITY AND RESOLUTION

For the purpose of our discussion, we will replace the usual terms ‘single-photon sensitivity’ and ‘single-photon resolution’ with ‘single-photoelectron sensitivity and resolution,’ to decouple the quantum efficiency of the photocathode from the consideration.

Single-photoelectron sensitivity is the ability of a photosensor to detect a single photoelectron unambiguously. Let us first recall that an ABALONE Photosensor converts a single photoelectron into about 55 detected secondary photons. The corresponding G-APD signal competes with noise, which is just the thermionic noise of the G-APD. Since the level of noise is below the single secondary-photon level, the signal to noise ratio for the detection of a single photoelectron is in our case well above 55. The probability to miss such a strong signal (false negative) is therefore negligible, just like the probability that noise would fluctuate to the 55-photon signal level (false positive). The single-photoelectron sensitivity of the ABALONE Photosensor would thus be perfect, should the energy of all photoelectrons be fully converted into secondary photons. That is not the case for all electrons, because about 30-40% of them back-scatter from the LYSO scintillator, after a fraction of their energy has been already converted into secondary photons. Some of those back-scattered electrons shortly return into LYSO after looping through vacuum, for their second detection, so their total energy is recorded. The others are recorded with reduced amplitudes, see the BS-pe peak in Fig.7, but these amplitudes are in most cases still much higher than the noise level. The single-photoelectron sensitivity is therefore practically perfect for most of the photoelectrons, including an estimated 80% of the non-returning back-scattered ones.

Single-photoelectron resolution is the precision with which a photosensor allows one to determine the number of photoelectrons from the measured signal amplitude. PMTs feature a notoriously poor, virtually nonexistent single-photoelectron resolution, because of the strong fluctuations in the first stage of the electron multiplication process ($\text{gain} < 5$). These fluctuations are amplified and further widened throughout the dynode chain. In contrast, the ABALONE Photosensor amplifies the single photoelectron signal in two steps, first, as explained above, through the acceleration of a photoelectron and the conversion of its energy into about 55 detected secondary photons, and second, the amplification of each of those photons in the G-APD with a

gain of 10^6 . The first process dominates statistical fluctuations that are narrow (10-15%) because of the high gain of 55.

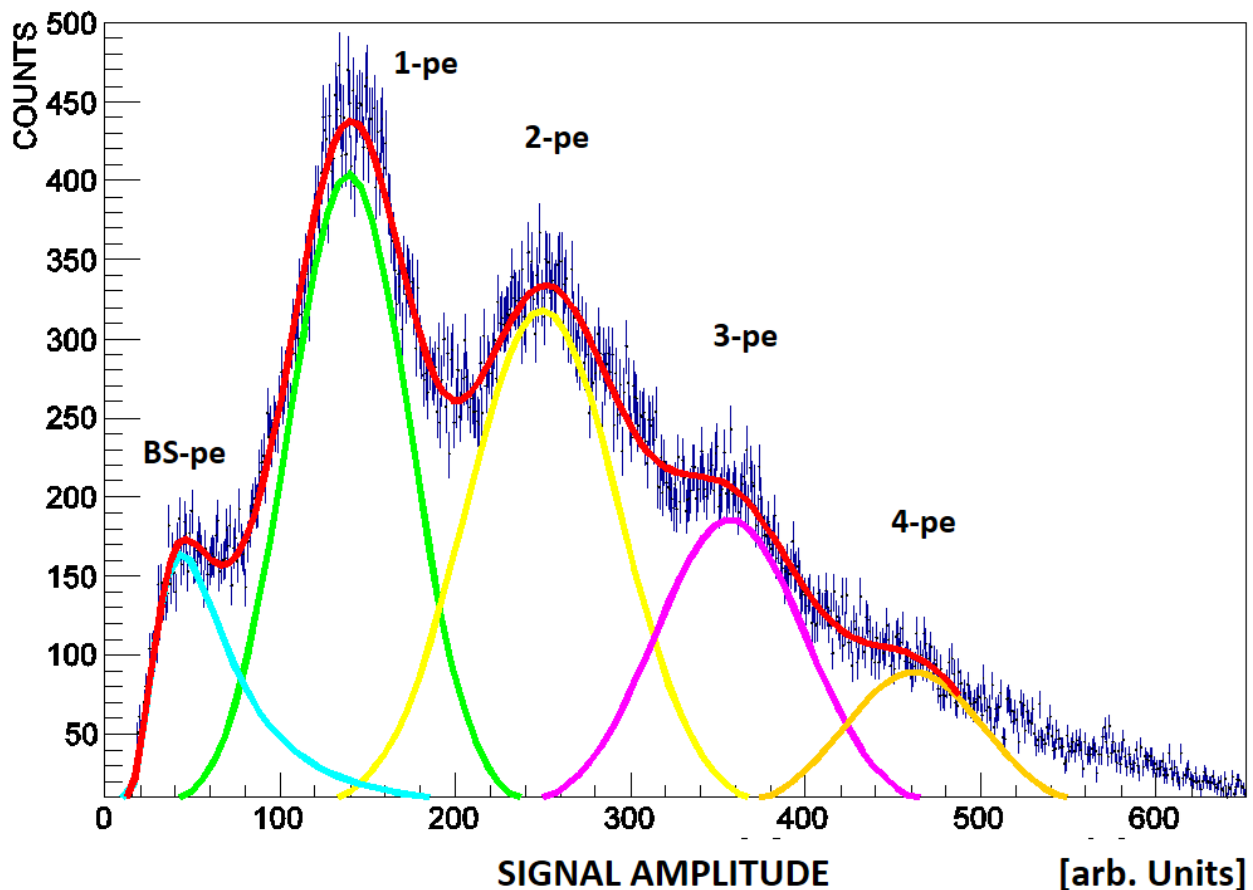


Fig.7 A typical amplitude spectrum taken at an acceleration potential of 23kV, with a slow signal of the 3x3mm² SensL-J G-APD, at a 28.5V bias voltage. Gaussian function components in the common fit represent photoelectron counts from 1 to 4, while the Landau function (BS-pe) represents the contribution of non-returning back-scattered single photoelectrons ($\chi^2/\text{ndf}=532/464$). The presented data were taken in coincidence with the light pulser and the pedestal events are virtually absent.

Fig.7 shows a typical signal amplitude spectrum, fitted with a sum of four Gaussian functions and a Landau function. Each Gaussian function corresponds to a specific number of photoelectron counts (1-4), while the Landau function stands for the asymmetric distribution of single back-scattered photoelectrons that did not return to the Windowlet. The situation becomes more complicated with combinations of fully detected and non-returning back-scattered electrons. For instance, for the class of events where one electron is fully detected and another one is back-scattered without returning, the amplitude distribution is a superposition of a full 1-pe peak and a BS-pe peak starting at the 1-pe peak position in Fig.7. A fraction of 2-photoelectron events thus appears within the 1-pe peak, and more so on its right side. Our fit clearly ignores such mixed contributions, so they are effectively shared among the neighboring Gaussian peaks, widening them significantly. The relative width of the 1-pe peak is $\sigma_{1\text{-pe}}/A_{1\text{-pe}}=24\%$, which is indeed very

narrow, but still wider than what would be ideally expected for pure 1-photoelectron signals without any widening (~15%).

For most of the practical purposes, a sharp cut between neighboring peaks in Fig.7 separates different photoelectron counts very efficiently. The level of single-photoelectron resolution achieved by the ABALONE Photosensor is unparalleled by any PMT. Further significant improvements (factor 2-3 increase in amplitude) to the single-photoelectron sensitivity and resolution are straightforward with the most recent generation of G-APDs and high-yield scintillators.

Deviations in the linearity of response to strong light pulses, both as a function of the light intensity and the acceleration potential, are a natural consequence of the G-APD saturation, which takes place when multiple secondary photons fall into a single G-APD cell. Recall that due to its Geiger-mode operation, a G-APD gives a standard signal, no matter how many photons enter a given cell. The dynamic range may be extended in three very simple ways: (i) by lowering the acceleration potential, (ii) by lowering the bias voltage, or (iii) by replacing the G-APD with another one that contains more cells.

5. SUMMARY

The unprecedentedly simple ABALONE Photosensor comprises only three vacuum-processed components, each made of glass. Through avoidance of all materials other than glass, this invention has bypassed the “Old-Technology Barrier” that has shackled the 80-year old photomultiplier tube (PMT) manufacture, as well as all of the other vacuum photosensor concepts (Smart-PMTs, HPDs and MCP-PMTs). The ABALONE Technology involves only standard mass-production techniques (rapid plasma cleaning, thin-film deposition, (robotic) transport and positioning within a continuous production line). This technology is equivalent to the production of blank CDs. We have produced ABALONE Photosensors in the custom-designed production line at UC Davis, and have tested them continuously since 2013.

We discuss the following key performance aspects: vacuum integrity and afterpulsing (two orders of magnitude better than in the best PMTs), timing resolution (well below 1ns), photoelectron collection efficiency (~100%), single-photoelectron sensitivity and resolution (separable photoelectron peaks), and photoelectron back-scattering. (Even additional significant improvements will be straightforward with the application of the latest G-APDs and fast, high-yield scintillators, and with certain modifications to the geometry of the ABALONE Photosensor).

The modern ABALONE Technology is far superior to prior art in performance, robustness and the capacity for integration into large-area detector shells. It is about two orders of magnitude more cost effective while being mass-producible with a relatively low investment. ABALONE Photosensors can open the doors for a new generation of large-area detectors in all application areas.

ACKNOWLEDGEMENTS

This project was partly supported by the UC Office of the President, under the Program UC Proof of Concept Award, Grant ID No. 247028 (2013-2014). The authors thank technicians David Hemer and Keeith Delong for devoted and professional work on this project. The authors also thank Bruno Ferenc Šegedin for writing assistance and language help, and Dan Ferenc Šegedin for proof-reading the article.

REFERENCES

1. Daniel Ferenc, U.S. Patent 9,064,678, 2010.
2. Daniel Ferenc, Patent pending, WO 2015/176000 A1, PCT/US2015/031188, 2014.
3. J. Todd, Journal of Applied Physics 26, 1238 (1955).
4. Daniel Ferenc, Andrew Chang, Leah Johnson, Daniel Kranich, Alvin Laille, Eckart Lorenz, A new method for vacuum sealing of flat-panel photosensors, Nuclear Instruments And Methods In Physics Research A 567(2006)205.
5. H. Bethe, Zur Theorie des Durchgangs schneller Korpuskularstrahlen durch Materie, Annalen der Physik, 397(1930)325.
6. Daniel Ferenc, Daniel Kranich, Alvin Laille, Eckart Lorenz, The Novel Light Amplifier Concept, Nuclear Instruments And Methods In Physics Research A 567(2006)166.
7. E. Lorenz, D. Ferenc, A New Readout Of Large Area Smart Photomultipliers By Geiger-Mode APDs, Nuclear Instruments And Methods In Physics Research A 572(2007)434.
8. R. Mirzoyan, D. Müller, J. Hose, U. Menzel, D. Nakajima, M. Takahashi, M. Teshima, T. Toyama, T. Yamamoto, Nuclear Instruments And Methods In Physics Research A 845(2017)603.
9. D. L. Smith, Thin Film Deposition, Mc Graw Hill (1995).
10. J. F. Ziegler, J. Biersack and U. Littmark, The Stopping and Range of Ions in Matter, Pergamon Press (1985).